PHILOSOPHICAL MAGAZINE B, 2000, VOL. 80, NO. 10, 1757–1772

The structural origin of broken chemical order in $GeSe_2$ glass

P. BOOLCHAND† and W. J. BRESSER

Department of Electrical and Computer Engineering and Computer Science, University of Cincinnati, Cincinnati, Ohio 45221-0030, USA

[*Received 26 April 2000 and accepted 3 May 2000*]

ABSTRACT

Raman scattering, ^{119}Sn Mössbauer spectroscopy and temperature-modulated differential scanning calorimetry experiments have been performed on $(Ge_{0.99}Sn_{0.01})_xSe_{1-x}$ glasses in the $0.30 < x < 0.36$ range. Both Raman and Mössbauer spectroscopies show that Ge–Ge signatures first appear near $x = 0.31(1)$, and their concentration slowly increases with increasing x to acquire a value of 1.92(30)% at $x = 1/3$, corresponding to $GeSe_2$ glass. Thereafter $(1/3 < x < 0.36)$ the concentration of these bonds increases precipitously with increasing x. Glass transition temperatures $T_g(x)$ reflect the connectivity of the network and are found to increase with increasing x; however, the rate dT_g/dx of T_g increase slows down markedly at (i) $x \geq 0.31(1)$, and the rate actually reverses sign (ii) at $x \geq 0.34$. Feature (i) coincides with nucleation and (ii) with precipitous growth of Ge–Ge signatures. These T_g trends show that the presence of Ge–Ge signatures decreases the global connectivity of the glasses. The results unequivocally demonstrate that the Ge–Ge bonds constitute part of a marginally rigid $Ge_2(Se_{1/2})_6$-bearing nanophase that is formed separately from the $Ge(Se_{1/2})_4$-tetrahedra-bearing backbone of the glasses.

§ 1. INTRODUCTION

The atomic-scale structure of glasses at a short range (less than 3 Å) and at a medium range (3–15 Å) often differs from those of their crystalline counterparts in subtle ways, and it is not always obvious how to decode those differences by merely examining the stoichiometric compositions in diffraction and spectroscopic experiments. Compositional trends in bond and site signatures can provide important clues on their microscopic origin. In general, these differences in structure stem from the fact that, in glasses, matter is structurally arrested at a lower density (or at higher molar volumes) than in crystals. New molecular structures that are stable at low or negative pressures can nucleate, leading to intrinsic differences in *local structure* and *medium-range structure* between glasses and crystals. Silica glass is a particularly interesting case. Diffraction experiments show that the narrow distribution of the O bridging angle between $Si(O_{1/2})_4$ tetrahedra in the crystalline phase (quartz) is replaced by a rather wide distribution (120–180°) in SiO_2 glass (Mozzi and Warren 1969). Within constraint counting algorithms (Phillips 1979, 1999), this element of

†Email: Punit.Boolchand@uc.edu.

Philosophical Magazine B ISSN 1364–2812 print/ISSN 1463–6417 online © 2000 Taylor & Francis Ltd
http://www.tandf.co.uk /journals

local structure represents the essential factor necessary to understand (Zhang and Boolchand 1994) the propensity of glass formation in this prototypical oxide. These differences in local structure also lead to profound differences in the medium-range structure as reflected in the distribution of n-membered $(SiO)_n$ rings (Galeener 1990, Elliott 1995, Kerner 1995) in fused silica with $n = 3, 4, 5, 7$ in addition to the usual $n = 6$ rings also found in the crystalline phases.

The molecular structure of $GeSe_2$ glass has enjoyed widespread interest over the past three decades (table 1). Historically, the structure of $GeSe_2$ glass in analogy to SiO_2 glass has also been described (Nemanich *et al.* 1983) as a chemically ordered continuous random network (COCRN) of $Ge(Se_{1/2})_4$ tetrahedral units. Unlike the case of O in silica, the Se bridging angle in $GeSe_2$ glass is actually reasonably well defined (Vashishta *et al.* 1989a,b, Susman *et al.* 1990, Cobb *et al.* 1996). Furthermore, local probes such as Raman scattering (Murase *et al.* 1983), ^{119}Sn (Boolchand *et al.* 1982) and ^{129}I Mössbauer spectroscopy (Bresser *et al.* 1981, 1986) measurements have all shown that the stoichiometric $GeSe_2$ bulk glass in contrast with its crystalline phases (high-temperature (α) and low-temperature (β) phases) is *not* completely chemically ordered. These local probes are very sensitive to the concentration of disordered bonds (Ge—Ge and Se—Se) and place their concentration near 2% in $GeSe_2$ glass. It was not until the full power of isotopic substitution was brought to bear that final confirmation was given (Pitri *et al.* 2000) of the presence of these chemically disordered bonds in $GeSe_2$ glass directly in neutron partial distribution functions recently. Because of the small concentration of homopolar bonds, the structure of the stoichiometric glass has often been assumed (Pitri *et al.* 2000, Elliott 1993) to be defected continuous random network (CRN).

In this work we present new Raman, ^{119}Sn Mössbauer spectroscopy and temperature-modulated differential scanning calorimetry (MDSC) results on $(Ge_{0.99}Sn_{0.01})_xSe_{1-x}$ glasses in the range $0.30 < x < 0.36$, with measurements performed on the same batch of samples. Composition trends in the spectroscopic signatures are found to be closely correlated to those in the glass transition temperature T_g. An important consequence of this correlation is that one can now distinguish whether Ge—Ge bonds form part of the tetrahedral network (backbone) or whether they coexist in a separate ethane-like $Ge_2(Se_{1/2})_6$ nanophase. New insights into the compositional trends of T_g have emerged from stochastic agglomeration theory (Kerner and Micoulaut 1994) which show that T_g provides a measure of global connectivity of a glass network. Qualitatively different $T_g(x)$ trends can be expected near $x = 1/3$ if Ge—Ge bonds form part of the tetrahedral backbone or alternatively separate into a Ge-rich nanophase. In the former case, $T_g(x)$ can be expected to continue to increase at $x > 1/3$ (as they do in the Si_xSe_{1-x} binary), reflecting the increasing global connectivity of the network. In the latter case, however, $T_g(x)$ would show a local maximum near $x = 1/3$ provided that the Ge-rich nanophase possesses a fixed but marginally rigid structure. Our experiments support the latter circumstance, suggesting that the stoichiometric glass is intrinsically phase separated on a molecular scale into Se-rich and Ge-rich regions.

§2. Experimental details

2.1. *Sample synthesis and thermal characterization*

Glasses were synthesized using 99.999% elemental Ge pieces and Se shots from Cerac, Inc. and isotopically enriched ^{119}Sn slivers in the elemental form as starting

Table 1. An historical perspective of results that bear on the molecular structure of $GeSe_2$ glass.

Method	Result	Reference
Raman scattering and neutron scattering	A_1 mode identified with CS tetrahedra; A_1 companion identified with mode of *n*-fold rings ($n = 4, 5, 6$)	Nemanich *et al.* (1977)
Raman scattering	A_1-companion identified as a mode of Se—Se cluster edge bonds; paracrystalline models of Ge-rich and Se-rich clusters proposed for $GeSe_2$ glass	Bridenbaugh *et al.* (1979)
^{129}I Mössbauer emission spectroscopy	Finite concentration of Se—Se bonds; internal surfaces native to $GeSe_2$ glass	Bresser *et al.* (1981)
^{119}Sn Mössbauer spectroscopy	Finite concentration of Ge—Ge bonds in $GeSe_2$ glass	Boolchand *et al.* (1982)
Raman scattering	246 cm^{-1} (bond-stretching) and 145 cm^{-1} (bond-bending) modes of Se—Se cluster edge bonds identified	Murase *et al.* (1983)
Raman scattering and neutron scattering	A_1 companion mode identified as mode of ES tetrahedra; glass structure described as a COCRN	Nemanich *et al.* (1983)
Raman scattering	A_1 and A_1 companion identified with CS and ES tetrahedra; glass structure described as a stochastic network	Sugai (1987)
Structure factor of $GeSe_2$ glass and liquid, measured by Susman *et al.* (1990), analysed using two- and three-body forces for a 648-atom model	Origin of the first sharp diffraction peak identified with Ge—Se and Ge—Ge correlations between 4 and 8 Å	Vashishta *et al.* (1989a,b)
Neutron structure factor of $GeSe_2$ glass and liquid	Glass structure composed of CS and ES tetrahedra, similar to that of α-$GeSe_2$	Susman *et al.* (1990)
Neutron partial distribution function measured in $GeSe_2$ using isotopic substitution	Finite concentration of homopolar bonds in liquid $GeSe_2$	Penfold and Salmon (1991)
Structure factor of $GeSe_2$ glass and liquid, measured by Susman *et al.* (1990), analysed using *ab-initio* molecular dynamics for a 216-atom model	Four- and six-membered ring correlations contribute to the first sharp diffraction peak. Vibrational and electronic densities of states calculated	Cobb and Drabold (1997); Cobb *et al.* (1996)
Structure factor and partial distribution functions of $GeSe_2$ liquid, measured by Penfold and Salmon (1991), analysed using *ab-initio* molecular dynamics for a 120-atom model	Liquid structure composed of regular $Ge(Se_{1/2})_4$ tetrahedra coexisting with homopolar bonds and threefold centres. Origin of the first sharp diffraction peak not clear	Massabrio *et al.* (1998)
Neutron partial distribution function measured in $GeSe_2$ glass using isotopic substitution	Finite concentrations of Ge—Ge and Se—Se bonds in $GeSe_2$ glass confirmed; high concentration of distorted CS $Ge(Se_{1/2})_4$ tetrahedra	Pitri *et al.* (2000)
Raman scattering, ^{119}Sn Mössbauer spectra and MDSC on Sn-doped Ge_xSe_{1-x} glasses performed on same samples	$T_g(x)$ variation correlated to Ge—Ge bond concentration; ethane units *not* part of the tetrahedral backbone	Present work

materials (Boolchand *et al.* 1982). Bulk glasses of $(Ge_{0.99}Sn_{0.01})_xSe_{1-x}$ composition at several stoichiometries spanning the $0.30 \leq x \leq 0.36$ range were synthesized by heating the starting materials in evacuated (5×10^{-7} Torr) quartz ampoules to 1000°C for at least 48 h (keeping the melts vertical), followed by an equilibration of melts 50°C above the liquidus temperature (Sarrach *et al.* 1976) for 6 h before a water quench.

Accurate values of T_g can be deduced using MDSC, a new more sensitive variant (Wunderlich *et al.* 1994, Wagner *et al.* 1997) of traditional differential scanning calorimetry (DSC). Not only are the scan rates used in MDSC ($3^\circ C\,min^{-1}$) an order of magnitude lower than those used in DSC ($20^\circ C\,min^{-1}$), but also MDSC

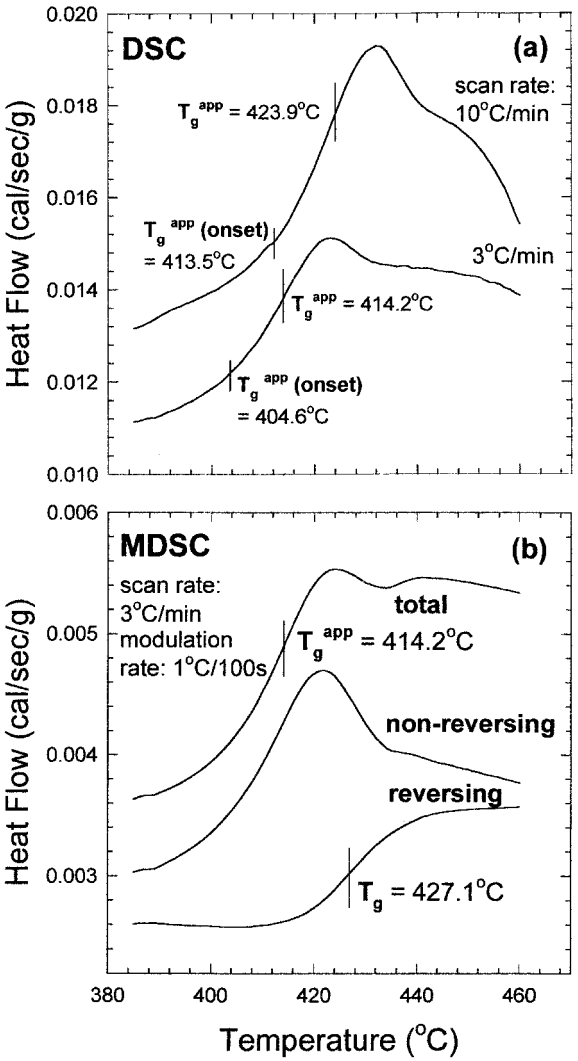

Figure 1. DSC and MDSC scans of $GeSe_2$ glass showing an apparent T_g of 424°C at a $10^\circ C\,min^{-1}$ scan rate and an apparent T_g of 414°C at a $3^\circ C\,min^{-1}$ scan rate. In the MDSC mode using a scan rate of $3^\circ C\,min^{-1}$ and a modulation rate of 1°C per 100 s, a T_g of 427°C is observed.

permits deconvoluting the *total heat flow* H_t into a *reversing component* H_r and a *non-reversing component* H_{nr} (Boolchand *et al.* 1999b). The former heat flow H_r tracks the temperature-modulations and provides a true measure of ΔC_p and T_g, while the latter heat flow H_{nr} captures the kinetic effects (Selvanathan *et al.* 1999, 2000) associated with changes in network configurations as a precursor to softening of the glass at T_g. Figure 1 displays scans of our $GeSe_2$ glass sample taken in the DSC and the MDSC modes using a TA Instruments, Inc., model 2920 MDSC. At $3^\circ C\,min^{-1}$ scan rate, T_g using the MDSC mode is found to be $427^\circ C$.

Figure 2 gives the observed $T_g(x)$ variation for the Ge_xSe_{1-x} binary. The $T_g(x)$ trend in the $0.31 < x < 0.36$ range shows (figure 3(*a*)) a maximum near $x = 0.34$. The slope, dT_g/dx inferred from the $T_g(x)$ trend shows (figure 3(*b*)) a maximum near $x = 0.31$, and it vanishes as x increases to 0.34. For comparison, we have included $T_g(x)$ results on the Si_xSe_{1-x} binary in figure 2 taken from the work of Selvanathan *et al.* (1999, 2000).

2.2. *Raman scattering results*

Figure 4 displays Raman scattering results on the glasses excited using the 647.1 nm line from a Kr-ion laser at 250 μW. The back-scattered radiation was analysed (Feng *et al.* 1997) using a triple-monochromator system (model T 64000 from Instruments S.A., Inc.), which was equipped with a microscope attachment and a charge-coupled device detector. One can discern growth in the scattering strength of the $180\,cm^{-1}$ mode due to ethane-like units (Lucovsky *et al.* 1977, Feltz *et al.*

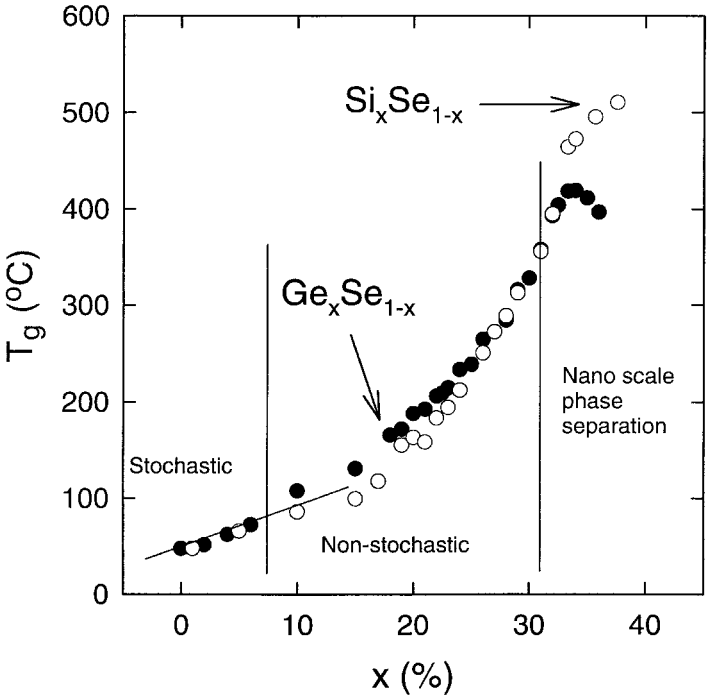

Figure 2. Observed T_g values in Ge_xSe_{1-x} glasses showing a linear increase at low x, and a maximum near $x = 0.34$. The linear increase at low x is in excellent accord with the predictions of slope equations (Kerner and Micoulaut 1994) corresponding to the straight line drawn.

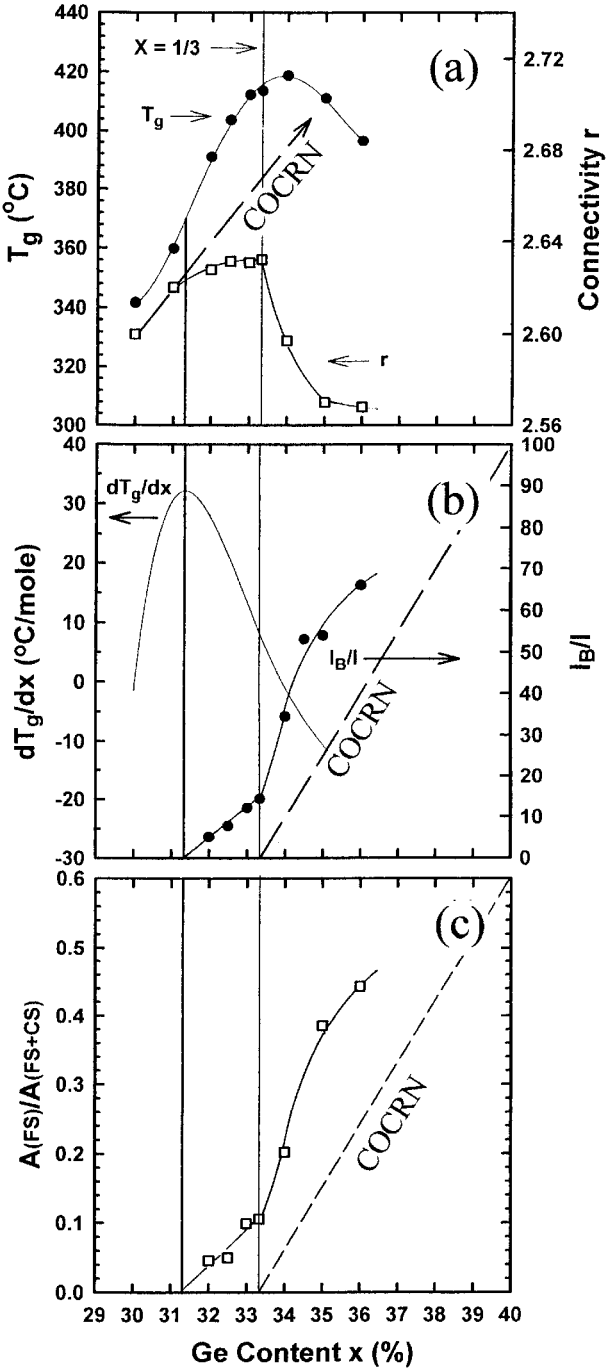

Figure 3. (*a*) Observed $T_g(x)$ trends and calculated $r(x)$ trends near $x = 0.34$ in the present binary; (*b*) observed dT_g/dx rate and Mössbauer I_B/I trends, (*c*) Raman $A(\mathrm{FS})/A(\mathrm{FS}+\mathrm{CS})$ trends deduced from spectra of figures 5 and 4. Note that the growth of B nanophase coincides with the maximum in dT_g/dx near $x = 0.31$ (thick vertical line). The broken lines give the expected linear variations in $r(x)$, I_B/I and $A(\mathrm{FS})/A(\mathrm{FS}+\mathrm{CS})$ for a chemically ordered continuous random network (COCRN).

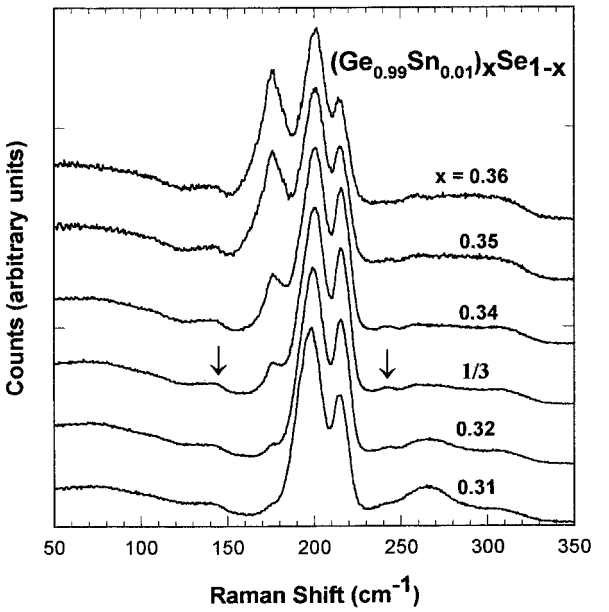

Figure 4. Raman line shapes in the indicated glasses showing the growth in scattering strength of the $180\,cm^{-1}$ which arises because the ethane-like units increase with increasing x. Vibrational modes of Se—Se cluster edge bonds are shown by arrows on the spectrum for $GeSe_2$ glass.

1977) starting at $x = 0.32$. The integrated scattering strength $A(\mathrm{FS})$ under the ethane-like or face-sharing (FS) mode normalized to the sum $A(\mathrm{FS}+\mathrm{CS})$ of the corner-sharing (CS) mode (at $202\,cm^{-1}$) and FS mode scattering strengths, that is $A(\mathrm{FS})/A(\mathrm{FS}+\mathrm{CS})$, is plotted as a function of x in figure 3(*c*). The results show a monotonic growth of ethane-like units in the network starting at $x \geq 0.31$, at first slowly ($0.31 < x < 0.33$) and then rapidly ($0.33 < x < 0.36$). At $x = 1/3$, corresponding to $GeSe_2$ glass, the scattering strength ratio of the ethane-like mode to CS mode, $A(\mathrm{FS})/A(\mathrm{CS}) = 0.12(2)$, while that of the edge-shaving (ES) mode to the CS mode, $A(\mathrm{ES})/A(\mathrm{CS}) = 0.43(3)$. The Raman cross-sections of these modes have recently been estimated by density functional theory in the local density approximation (Jackson *et al.* 1999) and yield $\sigma(\mathrm{FS}):\sigma(\mathrm{CS}):\sigma(\mathrm{ES})$ of 49.2 : 47.9 : 40.5 in units of ångström^4 per atomic mass unit. From these data, one arrives at the concentration ratio of ethane-like to CS units of 0.13(2) and the concentration ratio of ES to CS units of 0.50(3). There is one Ge—Ge bond and six Ge—Se bonds per ethane-like unit, and four Ge—Se bonds per CS unit and per ES unit. The degree of broken chemical order in $GeSe_2$, that is the concentration ratio of Ge—Ge to Ge—Se bonds suggested by these data is found to be 1.92(30)%.

2.3. *Mössbauer spectroscopy results*

Mössbauer spectra of the glasses were obtained at 4.2 K using ^{119m}Sn in $CaSnO_3$ as an emitter and are displayed in figure 5. The observed line shapes were analysed in terms of two pairs of doublets, one centred near $v = 1.50\,mm\,s^{-1}$ (site A) identified (Boolchand *et al.* 1982) with the tetrahedrally coordinated $Sn(Se_{1/2})_4$, and a second centred near $v = 2.5\,mm\,s^{-1}$ (site B) identified with a non-tetrahedrally coordinated

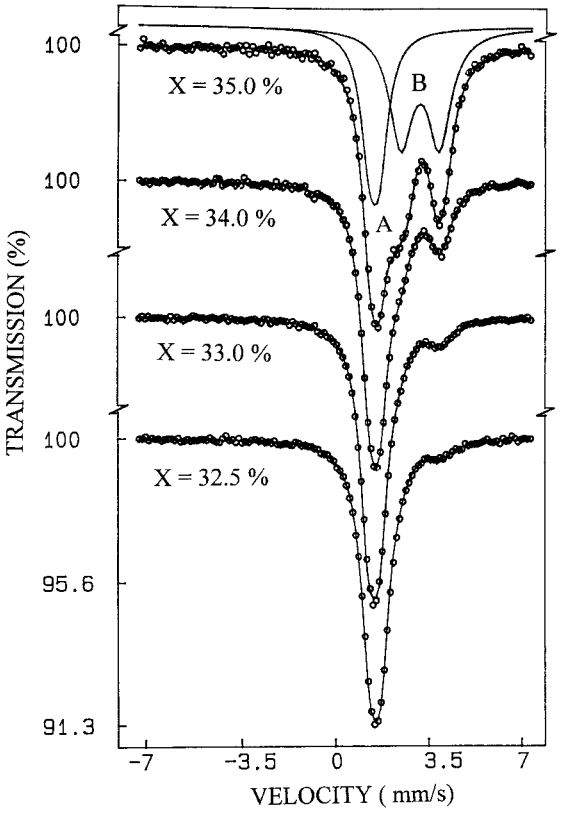

Figure 5. ^{119}Sn Mössbauer spectra of $(Ge_{0.99}Sn_{0.01})_xSe_{1-x}$ glasses at $x > 0.32$ showing that the intensity ratio I_B/I of the non-tetrahedral B site increases with increasing x.

species that results from the replacement of Ge by Sn in ethane-like units. The integrated site intensity ratios $I_B/(I_A + I_B) = I_B/I$ deduced from these Mössbauer measurements are plotted in figure 3(*b*). The site intensity ratios I_n/I (n = A, B) directly reflect the concentrations of the respective nanophases (A and B) in the network backbone, since the Lamb–Mössbauer factors of the two sites nearly equalize (Boolchand 2000a) as $T \rightarrow 0$ K. One finds that the Mössbauer site-intensity ratio I_B/I tracks the Raman scattering strength ratios $A(FS)/A(CS + FS)$, and I_B/I acquires a value of 0.14(1) at $x = 1/3$. Thus 14% of the Sn tracer atoms in $GeSe_2$ glass are non-tetrahedral. If we assume Sn to replace Ge sites randomly in ethane-like and CS units, then the concentration ratio N_{Ge-Ge}/N_{Ge-Se} of Ge—Ge bonds to Ge—Se bonds can be calculated and yields a value of 2.32(30)%. Both Raman scattering and Mössbauer spectroscopy yield the same degree of broken chemical order in the stoichiometric $GeSe_2$ glass, and place the concentration ratio of Ge—Ge bonds to Ge—Se bonds at 1.92(30)% and 2.32(20)% respectively.

Deconvolution of Raman line shapes becomes non-trivial when mode frequencies overlap, since neither mode widths nor mode intensities of a species in a glass are known *a priori*. There are two Raman-active modes of ethane-like units (Lucovsky *et al.* 1977): one at 180 cm^{-1} and a second at 202 cm^{-1}. The latter mode overlaps the mode of CS units. This has the fatal consequence that the observed ratio of the scattering strength of the 180 cm^{-1} mode to the sum of the scattering strengths of

the 180 and 200 cm^{-1} modes progressively underestimates (figure 3(*c*)) the degree of broken chemical order in the Ge_xSe_{1-x} glass system when the concentration of ethane-like units proliferates at $x > 0.34$. It is for this reason that at $x = 0.36$, for example, the broken chemical order deduced from Raman scattering experiments of 0.42 (figure 3(*c*)) underestimates the broken chemical order of the glass network (0.68) deduced from the Mössbauer effect experiments (figure 3(*b*)). In the Mössbauer effect experiments, ethane-like units contribute (figure 5) a symmetric doublet B whose contribution to the line shape can be uniquely deconvoluted even if there is an overlap with the singlet A ascribed to CS units because the line-shape function is known *a priori* and the symmetric nature of the doublet requires that both members of a quadrupole doublet have the same intensity.

§ 3. Discussion

3.1. *Compositional trends in T_g and nanoscale phase separation*

Although the nature of the glass transition continues to pose enormous challenges, considerable progress has been made in identifying the kinetic, thermal and structural factors that influence the magnitude of T_g. The T_g of a network-forming solid appears to be an intimate reflection of its global connectivity. Recently, new ideas to understand T_g as a function of network connectivity, or mean coordination number $\bar{r}$, were introduced using the stochastic agglomeration theory (Kerner and Micoulaut 1994) and slope equations. Parameter-free predictions of $T_g(r)$ trends in binary, ternary and quaternary chalcogenides have been made using slope equations (Micoulaut and Naumis 1999). For a IV–VI glass system such as the Ge_xSe_{1-x} binary, the slope equations predict $dT_g/dx = T_0/\ln 2$. The observed T_g trend at low values of x, $(0 < x < 0.08)$, closely matches the slope equation prediction, as shown in figure 1. T_0 represents the glass transition of Se glass. These results suggest that a stochastic or random network description appears appropriate for glasses possessing low connectivity. In contrast, at higher x $(x > 0.10)$, deviations set in as predicted T_g values are found to be systematically lower than the observed T_g values, probably because the configurational entropy of the network is lowered when select chemical configurations are energetically preferred. These results reflect the non-stochastic nature (Bresser *et al.* 1986) of the backbone emerging at higher x, in which specific rigid moieties form and eventually percolate at the rigidity transitions ($x = 0.20$ and $x = 0.23$) as discussed elsewhere (Boolchand *et al.* 1999). The importance of chemistry and network packing in melts of marginally rigid $(0.20 < x < 0.23)$ and rigid $(x > 0.23)$ networks apparently leads to growth of medium-range structure, and eventually to phase separation of the backbone on a nanoscale at $x > 0.31$ as discussed next.

In a defected-CRN model of Ge_xSe_{1-x} glasses, Ge—Ge bonds form as part of the network, and one expects the connectivity of the glass network to increase linearly (broken line in figure 3(*a*)) with x. Here $\bar{r} = 2(1 + x)$, since Ge and Se possess r values, of 4 and 2 respectively. There would be no reason for T_g values to decrease at $x > 1/3$, if indeed the connectivity of the backbone were to increase continuously. On the other hand, the T_g maximum near $x = 1/3$ is reminiscent of the liquidus temperature $T_\ell(x)$ maximum in the equilibrium phase diagram (Sarrach *et al.* 1976). These results suggest that glasses and corresponding melts near $x = 1/3$ are both phase separated into a tetrahedrally coordinated majority phase (A) and a

Ge-rich minority nanophase (B) (Boolchand *et al.* 1983). These ideas on phase separation can now be made quantitative using constraint-counting algorithms.

Perhaps the simplest assumption to make is that ethane-like units form part of zigzag-chain fragments rather than linear chains in a glass. This would require that the Se bridging bond angle with nearest-neighbour Ge atoms display some distribution, and we suppose that the underlying Se bond-angle constraint is intrinsically broken. Enumeration of both bond-stretching ($n_\alpha = r/2$) and bond-bending ($n_\beta = 2r - 3$) constraints for fourfold coordinated ($r = 4$) Ge, but only the bond-stretching constraint (n_α) for twofold-coordinated ($r = 2$) Se yields the number n_c of constraints per atom in a Ge_2Se_3 formula unit:

$$5n_c = 2\{[n_\alpha(\mathrm{Ge}) + n_\beta(\mathrm{Ge})] + 3n_\alpha(\mathrm{Se})\} \tag{1}$$

or

$$n_c = 3.40.$$

The mechanically effective coordination r_B describing the connectivity of the B nanophase then follows by requiring that

$$n_c = \tfrac{5}{2} r_B - 3 \tag{2}$$

and gives $\bar{r}_B = 2.56$. Thus, we find that the connectivity of the B nanophase is *less* than the maximum connectivity of the A nanophase with $\bar{r}_A = 2.67$.

In the $0 < x < 0.31$ range, $T_g(x)$ increases because the connectivity of the Ge cross-linked Se_n-chain network (A nanophase) increases linearly ($r_A = 2(1 + x)$) with increasing x. However, at $x \geq 0.31$, only a part of the excess Ge enters the A nanophase, with the rest nucleating the marginally rigid B nanophase ($\bar{r}_B = 2.56$), as revealed by our spectroscopic results (figures 3 (*b*) and (*c*)). The loss in global connectivity of the network upon nucleation of the B nanophase leads to a maximum in the slope dT_g/dx at $x = 0.31$ because the rate of T_g increase slows down thereafter. One can calculate the mean connectivity $\bar{r}$, of the backbone in terms of its constituent nanophases by writing

$$\bar{r} = n_A \bar{r}_A + n_B \bar{r}_B, \tag{3}$$

subject to the phase separation condition

$$\mathrm{Ge}_x\mathrm{Se}_{1-x} = n_B(\mathrm{Ge}_{0.4}\mathrm{Se}_{0.6}) + n_A(\mathrm{Ge}_t\mathrm{Se}_{1-t}). \tag{4}$$

Here n_A and n_B designate the concentrations of the A and B nanophases respectively in the backbone. Using equation (4), equation (3) can be rewritten as follows:

$$\bar{r} = 2(1 + x) - 0.24 n_B(x). \tag{5}$$

The first term in equation (5) reflects the growth in connectivity of the backbone due to the A nanophase while the second term gives the loss of connectivity due to nucleation and subsequent growth of the B nanophase. Taking the concentration of the B nanophase, $n_B(x) = I_B/I$, from the Mössbauer effect results (figure 3 (*b*)), we have projected the $\bar{r}(x)$ variation of the $\mathrm{Ge}_x\mathrm{Se}_{1-x}$ backbone in figure 3 (*a*), and find a local maximum in $\bar{r}(x)$ that mimics the $T_g(x)$ (figure 3 (*a*)) maximum.

Near $x = 1/3$, the connectivities of the A and B phases are quite close to each other ($r_A = 2.60; r_B = 2.56$), suggesting that their T_g values must also be nearly the same. For these reasons, it is not possible to resolve the two T_g values as was possible in the Ag–Ge–Se ternary (Mitkova *et al.* 1999). In the Se-rich region of the ternary, a

Ag additive phase separates as a Ag_2Se glass ($T_g^1 = 230^\circ C$) phase, leaving behind a Se-deficient base glass ($T_g^2 = 100$–$350^\circ C$) with widely different connectivities.

3.2. *Molecular structure of $GeSe_2$ glass*

Structural studies on this binary glass have had a long and contentious history (table 1). It is comforting to see finally a convergence of views on the structure of $GeSe_2$ glass between the recently reported diffraction (Pitri *et al.* 2000), and the present Raman and Mössbauer spectroscopy results. The ratio of ES to CS tetrahedra in $GeSe_2$ glass, directly accessible in Raman scattering (§ 2.2), yields a value of 0.50(3). The result is in reasonable accord with the recent value of 34(5)/81(14) from the diffraction result of Pitri *et al.* (2000), and a value of 32/68 deduced by Vashishta *et al.* (1989a,b) from a molecular dynamics simulation of the measured structure factor results of Susman *et al.* (1990). On the other hand, the ratio of ES to CS tetrahedra equals 1.0 in α-$GeSe_2$ (Dittmar and Schäfer 1975, 1976) and zero in β-$GeSe_2$.

The present spectroscopic probes place the concentration of Ge—Ge bonds in $GeSe_2$ glass at a mean value of 2.12(30)%. This spectroscopic value is less than the value of 3.7(1.5)% reported in diffraction measurements (Pitri *et al.* 2000). The glass transition T_g(onset) of 394(6)°C reported by Pitri *et al.* (2000) for their $GeSe_2$ glass sample is somewhat lower than the T_g(onset) of 413(2)°C of our $GeSe_2$ glass samples measured under identical scanning conditions ($10^\circ C\,min^{-1}$) in DSC (figure 1). These T_g results suggest the possibility that the $GeSe_2$ glass samples used by Pitri *et al.* are slightly phase separated. For example, a concentration of Ge—Ge bonds larger by a factor of two would result if $x \approx 0.338$ instead of $x = 0.333$, since the concentration of such bonds (figure 3(*b*)) increases rather rapidly at $x > 1/3$. The melt-quench temperature of 850°C employed by Pitri *et al.* (2000) is high; it exceeds the liquidus (Sarrach *et al.* 1976) by 108°C and could be the reason for the slight phase separation of their $GeSe_2$ glass samples.

On strictly stoichiometric grounds, the presence of a finite concentration of Ge—Ge bonds in $GeSe_2$ glass requires the occurrence of Se—Se bonds. Experimental evidence for existence of Se—Se bonds in the stoichiometric glass first emerged from ^{129}I Mössbauer emission spectroscopy measurements in the early 1980s (Bresser *et al.* 1981, 1986). In the observed line shape, one could resolve contributions of Te-substituted Se—Se signatures from those of Te-substituted Ge—Se signatures because of the widely different nuclear quadrupole couplings at the daughter I atoms. The real surprise in these measurements, however, is that the contribution of Te-substituted Se—Se bonds is nearly twice those of Te-substituted Ge—Se bonds, even though the concentration of Se—Se bonds is a miniscule fraction of Ge—Se bonds. These experimental results constitute strong support for Se—Se signatures to dress surfaces of characteristic clusters in $GeSe_2$ glass. The oversized dopant (Te) atoms can then segregate at cluster edge sites and satisfy their bonding requirements by locally relaxing in the intercluster region with accumulation of little or no strain. The surface or edge segregation results in a twentyfold enhancement of the signal due to Te-substituted homopolar (Se—Se) bonds in relation to the Te-substituted heteropolar (Ge—Se) bonds (Boolchand 1985). Such an enhancement will be understandably precluded in a defected CRN model of this glass, since Te occupancy of both the Ge—Se and Se—Se intra-network bonds will result in accumulation of stress. These local probe results unequivocally support the existence of Se-rich internal surfaces native to the structure of the stoichiometric glass and are in harmony with

phase separation of the network into Se-rich and Ge-rich regions. The signature of Se—Se bonds in $GeSe_2$ glass has also been identified in Raman scattering measurements. These are the weak features observed at 246 and 145 cm^{-1} (see arrows in figure 4), which represent (Murase *et al.* 1983, Murase 2000) stretching and bending vibrational modes respectively.

A phase-separated model of the stoichiometric glass consisting of Se-rich and Ge-rich clusters was first proposed several years ago (Bridenbaugh *et al.* 1979). In this model, the Se-rich cluster was visualized as a two-chain wide fragment of the layer structure of α-$GeSe_2$ bordered by Se—Se bonds, while the Ge-rich cluster consisted of ethane-like units. The fraction N_{Ge-Ge}/N_{Se-Ge} of chemically disordered bonds, expected for the model works out to be 1/7 or 14.3%, which is a factor of seven larger than the experimentally measured value 2.12(30%). The smaller degree of broken chemical order measured in $GeSe_2$ glass suggests a higher degree of network polymerization, that is larger Se-rich clusters. Furthermore, the ratio of ES to CS tetrahedra in $GeSe_2$ glass as revealed by Raman and diffraction methods is nearly half the value in α-$GeSe_2$. The results suggest that Se-rich clusters in the glass in relation to the layers of α-$GeSe_2$ possess a substantially higher concentration of CS units and lead to a structure that is less compactly packed in which a significant concentration of distorted tetrahedra can occur (Pitri *et al.* 2000). These results are also consistent with the substantial reduction in the concentration of 16-membered rings in the glass in relation to α-$GeSe_2$ (Vashishta *et al.* 1989a,b). These large rings are formed in α-$GeSe_2$ layers and include chain segments of CS units intercepted by two pairs of ES units. Nevertheless, vestiges of the layers consisting of four-membered rings (ES units) and six-membered rings (formed at the cross-links of chains of CS units and ES units) appear to be largely intact in the glass structure (Vashishta *et al.* 1989a,b, Cobb and Drabold 1997) and may well be responsible for the elements of medium-range structure contributing to the first sharp diffraction peak (table 1). Thus, apart from these important structural differences between Se-rich clusters in the glass and the two-dimensional structure of α-$GeSe_2$, the principle of phase separation of the stoichiometric glass into Ge-rich and Se-rich clusters (Bridenbaugh et al. 1979) appears to be clearly upheld by the ^{129}I Mössbauer spectroscopy results and the local maximum in T_g near $x = 1/3$. Decoding the morphological structure of this prototypical glass in the end has thus required, in addition to spectroscopic and diffraction results, a clear interpretation of the glass transition temperature variation.

3.3. *Absence of nanoscale phase separation in $SiSe_2$ glass*

In Raman scattering of Si_xSe_{1-x} glasses a mode is observed at 200 cm^{-1} in Si-rich glasses ($x > 1/3$) and is identified with Si—Si signatures (Griffiths *et al.* 1984) associated with face-sharing $Si_2(Se_{1/2})_6$ tetrahedra. The scattering strength of the mode increases linearly with increasing $(x - 1/3)$. At the stoichiometric composition $x = 1/3$, there is no measurable evidence of Si—Si signatures (Selvanathan *et al.* 1999, 2000) in Raman scattering. The single bond strength difference ΔE, between corresponding heteropolar (Si—Se and Ge—Se) and homopolar (Si—Si and Ge—Ge) bonds (Pauling 1960) and T_g values of $GeSe_2$ and $SiSe_2$ glass are summarized in table 2. These data can be used to estimate the expected degree of broken chemical order based on the law of mass action. For $SiSe_2$ glass, the absence of any measurable broken chemical order is in good accord with the prediction of the law of mass action. For $GeSe_2$ glass, on the other hand, the observed broken

Table 2. The single-bond energy differences ΔE between heteropolar (X—Se) and homopolar (X—X) bonds (X = Si, Ge), T_g values deduced from MDSC using a $3^\circ C\,min^{-1}$ scan rate and a $1^\circ C$ per 100 s modulation rate, expected concentrations of homopolar bonds, and measured broken chemical orders in $SiSe_2$ and $GeSe_2$ glasses.

Glass system	ΔE^a (kcal mol^{-1})	$T_g(^\circ C)$	$\exp(-\Delta E/kT_g)$	Measured[b] broken chemical order
$SiSe_2$	9.2	464	2×10^{-3}	$< 10^{-3}$
$GeSe_2$	11.5	424	2×10^{-4}	2.1×10^{-2}

[a] $\Delta E = E_{X-Se} - E_{X-X}$, for X = Si, Ge.
[b] Fraction N_{X-X}/N_{X-Se} of bonds at X = Si, Ge.

chemical order exceeds the predicted value by two orders of magnitude. These results directly reflect the qualitative difference in distribution of homopolar bonds in these two stoichiometric glasses. Homopolar (Si—Si) bonds apparently form part of the backbone of Si_xSe_{1-x} glasses at $x > 1/3$, but Ge—Ge bonds are excluded from the backbone of Ge_xSe_{1-x} glasses already at $x > 0.31$. This particular element of structure appears to be driven by the difference in size of the two cations, one (Si) smaller than Se and the other (Ge) nearly equal to that of Se. These considerations lead not only to differences in the degree of broken chemical order at the stoichiometric composition in the two glass systems, but also to network connectivities, which is reflected in the widely different T_g trends (Boolchand 2000a) at $x > 1/3$. Thus, for example, in Ge_xSe_{1-x} glasses, the $T_g(x)$ values are found to display a threshold behaviour near $x = 1/3$, while, in Si_xSe_{1-x} glasses, the T_g values continue to increase in the $1/3 < x < 0.38$ range (figure 2). The latter constitutes evidence for the absence of a nanoscale phase separation in Si-rich ($x > 1/3$) Si_xSe_{1-x} glasses and is the exception that proves the rule. One would be hard pressed to understand these sharply contrasting trends in $T_g(x)$ between the two binaries based on mean chemical bond-strengths ($\bar{E}_b$) alone, given that in both binary glasses $\bar{E}_b$ decreases by nearly the same amount, ΔE (table 1), at $x > 1/3$.

Ge_2Se_3 glass consists of two nanophases, one consisting of ethane-like units (Feltz *et al.* 1977, Lucovsky *et al.* 1977), and a second consisting of distorted rocksalt units (Boolchand *et al.* 1983). Occurrence of ethane-like units in Ge_xSe_{1-x} melts and glasses at $x = 2/5$ and at $x = 1/3$ but not in corresponding crystals emphasizes in a rather direct manner how glasses differ from their crystalline counterparts. The ethane-like nanophase apparently represents a low-pressure molecular structure. It is populated in the glasses and plays a central role in determining glass formation in this binary for x extending up to 0.43 (Boolchand 2000b) since it is marginally rigid.

3.4. *Molecular structure of evaporated $GeSe_2$ films*

Evaporated thin films of $GeSe_2$ deposited on room-temperature substrates are non-crystalline. Such films have been examined in Raman scattering (Nemanich *et al.* 1978) and Mössbauer spectroscopy (Boolchand *et al.* 1987) experiments. As-deposited (virgin) films at normal incidence ($\alpha = 0$) possess a fragmented molecular structure in which the size of Ge-rich and Se-rich clusters can be expected to be qualitatively small, leading then to a substantial broken chemical order. The relevance of these experiments to the present work is that they permit a direct confirmation of Ge—Ge and Se—Se bond signatures in $GeSe_2$ glass. As expected, the $180\,cm^{-1}$ mode due to Ge—Ge signatures (ethane-like units) and the 246 and

145 cm^{-1} modes due to Se—Se bond stretching and bond bending are all qualitatively enhanced in the evaporated films in relation to the bulk glass. Furthermore, when virgin films are thermally annealed, the network polymerizes, and the concentrations of Se—Se and Ge—Ge signatures reduce qualitatively to approach values characteristic of the bulk glass.

The ^{119}Sn Mössbauer spectroscopy results on thin films are more quantitative than Raman scattering data and have permitted a measurement of the underlying activation energies (Boolchand *et al.* 1987) in thermal annealing studies. By examining the (annealing) temperature dependence of the broken chemical order (I_B/I), activation energies for the chemical ordering process have been established. The magnitudes of the bimodal activation energies (74(5) and 150(15) meV) suggest that the physical process underlying growth of chemical order involves the formation of heteropolar bonds (Ge—Se) at the expense of homopolar bonds (Ge—Ge and Se—Se) by a correlated motion of large group of atoms (molecular clusters) rather than single atom diffusion (0.7 eV) as reported in tracer diffusion experiments (Eichorn and Frischat 1978) on chalcogenide glasses.

Recently we have examined the molecular structure of obliquely deposited ($\alpha \neq 0$) $GeSe_2$ films (Chopra *et al.* 1981) in Raman scattering and ^{119}Sn Mössbauer spectroscopy experiments (Boolchand *et al.* 1999a). The results show that nanoscale phase separation effects in as-deposited films increase qualitatively with increasing obliqueness angle α and are reflected in the high porosity and subsequent growth of columns when $\alpha = 80^\circ$ (Chopra *et al.* 1981). The results will be discussed in a forthcoming publication.

3.5. *Optical bandgap in Ge_xSe_{1-x} glasses near $x = 1/3$*

The nanoscale phase separation model of $GeSe_2$ also provides a good basis to account for the local maximum in the optical bandgap E_g near $x = 1/3$ in the present binary. A fully cross-linked A nanophase consisting of Ge—Se bonds can be expected to have an intrinsically larger optical gap than the gap of the B nanophase in which weaker Ge—Ge bonds proliferate. It has been suggested (Tanaka 1989) that the threshold behaviour in several physical properties including E_g near $\bar{r} = 2.67$ may constitute evidence of rigidity of layer-like structures percolating in three dimensional networks. In the present binary, the envisaged transition is likely to be completely masked by the gross chemical phase separation effects that exist near $r = 2.67$. The suggested transition, if it exists, can perhaps be isolated in glass systems where nanoscale phase separation effects are suppressed owing to chemical disorder, as in the $Ge_xAs_ySe_{1-x-y}$ ternary at $x = y$ when $T_g(r)$ variation is found (Boolchand 2000a) to increase almost linearly in the $2 < \bar{r} < 2.7$ range.

3.6. *Boson peak scattering strength in Ge_xSe_{1-x} glasses near $x = 1/3$*

The microscopic origin of the boson peak in glasses continues to be a subject of current discussions. Some of the discussion has focused on the role of dopants (Tikhomirov *et al.* 1999) in enhancing the scattering strength of the boson peak in network glasses, while in other cases the emphasis has been on the functional form of the line shape (Nakamura *et al.* 1998) used to analyse the observed peak and the interpretation of the peak frequency in the base glass. It appears that a common feature of most discussions in this regard is that the excitation is intrinsically related to the heterogeneity of the glass structure. In a recent publication, Boukenter and Duvall (1998) have reported on the boson peak in bulk Ge_xSe_{1-x} glasses and noted

the existence of a local maximum in scattering strength of this mode near $x = 0.34$. A natural interpretation of the boson peak intensity maximum in Ge_xSe_{1-x} glasses near $x = 0.34$ would appear to be the intrinsic nanoscale phase separation that we have eluded to in this work. It would be of interest to compare and contrast boson peak scattering results on the Ge–Se binary with those on the Ge–As–Se ternary.

§ 4. Conclusions

Raman scattering and Mössbauer spectroscopy experiments on Ge_xSe_{1-x} glasses place the concentration of homopolar bonds at 2.12(30)%, in reasonable accord with recent diffraction results. Compositional trends in T_g provide new insights into the distribution of these homopolar bonds. The maximum in T_g near $x = 0.34$ in Ge_xSe_{1-x} glasses constitutes evidence for chemical phase separation of the backbone into two types of nanostructure: a Se-rich majority $Ge(Se_{1/2})_4$ phase and a minority Ge-rich $Ge_2(Se_{1/2})_6$ nanophase. The present ideas can be expected to extend generally to other binary chalcogenide glasses such as Ge_xS_{1-x} and As_ySe_{1-y} that also reveal a threshold in T_g near $x = 1/3$ and $y = 2/5$ respectively and would thus appear to be nanophase separated as well.

Acknowledgements

It is a pleasure to acknowledge discussions with R. Kerner, M. Micoulaut, J. C. Phillips, D. Drabold and K. Jackson. This work is supported by National Science Foundation grant DMR-97-01289.

References

Boolchand, P., 1985, *Physical Properties of Amorphous Materials*, edited by D. Adler, B. B. Schwartz, and M. C. Stelle (New York: Plenum) p. 221.
Boolchand, P., 2000a, *Asian J. Phys.*, **9**, 199.
Boolchand, P. (editor), 2000b, *Insulating and Semiconducting Glasses* (Singapore: World Scientific), pp. 191–247.
Boolchand, P., Bresser, W. J., and Chopra, K. L., 1999a, *Bull. Am. phys. Soc.*, **44**, 1434.
Boolchand, P., Enzweiler, R. N., and Tenhover, M., 1987, *Diffusion Defect Data*, **53–54**, 415.
Boolchand, P., Feng, X., Selvanathan, D., and Bresser, W. J., 1999b, *Rigidity Theory and Applications*, edited by M.F. Thorpe and P. M. Duxbury (New York: Kluwer–Plenum), chapter 5b, pp. 279–295.
Boolchand, P., Grothaus, J., Bresser, W. J., and Suranyi, P., 1982, *Phys. Rev.* B, **25**, 2975.
Boolchand, P., Grothaus, J. G., and Phillips, J. C., 1983, *Solid St. Commun.*, **45**, 183.
Boukenter, A., and Duval, E., 1998, *Phil. Mag.* B, **77**, 557.
Bresser, W. J., Boolchand, P., and Suranyi, P., 1986, *Phys. Rev. Lett.*, **56**, 2493.
Bresser, W. J., Boolchand, P., Suranyi, P., and de Neufville, J. P., 1981, *Phys. Rev. Lett.*, **46**, 1689.
Bridenbaugh, P. M., Espinosa, G. P., Griffiths, J. E., Phillips, J. C., and Remeika, J. P., 1979, *Phys. Rev.* B, **20**, 4140.
Chopra, K. L., Harshavardhan, S. K., Rajgopalan, S., and Malhotra, L. K., 1981, *Solid St. Commun.*, **40**, 387.
Cobb, M., and Drabold, D., 1997, *Phys. Rev.*, **56**, 3054.
Cobb, M., Drabold, D. A., and Cappelletti, R. L., 1996, *Phys. Rev.* B, **54**, 12 162.
Dittmar, G. V., and Schäfer, X., 1975, *Acta crystallogr.* B, **31**, 2060.
Dittmar, G. V., and Schäfer, X., 1976, *Acta crystallogr.* B, **32**, 1188.
Eichorn, V., and Frischat, G. H., 1978, *J. non-crystalline Solids*, **30**, 211.
Elliott, R., 1995, *J. non-crystalline Solids*, **182**, 1.

ELLIOTT, S. R., 1993, *Glasses and Amorphous Materials*, edited by J. Zarzycki (New York: VCH), p. 377.
FELTZ, A., ZICKMULLER, H., and PFAFF, G., 1977, *Amorphous and Liquid Semiconductors*, edited by W.E. Spear (Centre for Industrial Consultancy and Liason, University of Edinburgh), p. 125.
FENG, X., BRESSER, W. J., and BOOLCHAND, P., 1997, *Phys. Rev. Lett.*, **78**, 4422.
GALFEENER, F. L., 1990, *J. non crystalline Solids*, **123**, 182.
GRIFFITHS, J., MALYJ, M., ESPINOSA, G. P., and REMEIKA, J. P., 1984, *Phys. Rev.* B, **30**, 6978.
JACKSON, K., BRILEY, A., GROSSMAN, S., POREZAG, D. V., and PEDERSON, M. R., 1999, *Phys. Rev.* B, **60**, 14985.
KERNER, R. 1995, *J. non-crystalline Solids*, **182**, 9.
KERNER, R., and MICOULAUT, M., 1994, *J. non-crystalline Solids*, **176**, 271.
LUCOVSKY, G., NEMANICH, R. J., and GALEENER, F. L., 1977, *Amorphous and Liquid Semiconductors*, edited by W.E. Spear (Centre for Industrial Consultancy and Liason, University of Edinburgh), p. 130.
MASSSOBRIO, C., PASQUERELLO, A., and CAR, R., 1998, *Phys. Rev. Lett.*, **80**, 2342.
MICOULAUT, M., and NAUMIS, G., 1999, *Europhys. Lett.*, **47**, 568.
MITKOVA, M., WANG, Y., and BOOLCHAND, P., 1999, *Phys. Rev. Lett.*, **83**, 3848.
MOZZI, R. L., and WARREN, B. E., 1969, *J. Appl. Crystallogr.* **2**, 164.
MURASE, K., 2000, *Insulating and Semiconducting Glasses*, edited by P. Boolchand (Singapore: World Scientific, chapter 6C, pp. 415–463.
MURASE, K., FUKUNAGA, T., YAKUSHIJI, K., YOSHIMI, T., and YUNOKI, I., 1983, *J. non-crystalline Solids*, **59–60**, 883.
NAKAMURA, M., MATSUDA, O., and MURASE, K., 1998, *Phys. Rev.* B, **57**, 10 228.
NEMANICH, R. J., CONNELL, G. A. N., HAYES, T. M., and STREET, R. A., 1978, *Phys. Rev.* B, **18**, 6900.
NEMANICH, R. J., GALEENER, F. L., MIKKELSEN, J. C., CONNELL, G. A. N., ETHERINGTON, G., WRIGHT, A. C., SINCLAIR, R. N., 1983, *Physica*, B, **117–118**, 959.
NEMANICH, R. J., SOLIN, S. A., LUCOVSKY, G., 1977, *Solid St. Commun.*, **21**, 273.
PAULING, L., 1960, *The Nature of the Chemical Bond* (New York: Cornell University Press), p. 85.
PENFOLD, I. T., and SALMON, P. S., 1991, *Phys. Rev. Lett.* **67**, 97.
PHILLIPS, J. C., 1979, *J. non-crystalline Solids*, **34**, 153; 1999, *Rigidity Theory and Applications*, edited by M. F. Thorpe and P. M. Duxbury (New York: Kluwer–Plenum) pp. 155–171.
PITRI, I., SALMON, P. S., and FISCHER, H. E., 2000, *Phys. Rev. Lett.*, **84**, 2413.
SARRACH, D. J., DENEUFVILLE, J. P., and HAWORTH, W. L., 1976, *J. non-crystalline Solids*, **22**, 245.
SELVANATHAN, D., BRESSER, W. J., and BOOLCHAND, P., 2000, *Phys. Rev.* B, **61**, 15061.
SELVANATHAN, D., BRESSER, W. J., BOOLCHAND, P., and GOODMAN, B., 1999, *Solid St. Commun.*, **111**, 619.
SUGAI, X., 1987, *Phys. Rev.* B, **35**, 1345.
SUSMAN, S., VOLIN, K. J., MONTAGUE, D. G., and PRICE, D. L., 1990, *J. non-crystaline Solids*, **125**, 168.
TANAKA, K. E., 1989, *Phys. Rev.* B, **39**, 1270.
TIKHOMIROV, V. K, JHA, A., PERAKIS, A., SARANTOPOULOU, E., NAFTALY, M., KRASTEVA, V., LI, R., and SEDDON, A. B., 1999, *J. non-crystalline Solids*, **256–257**, 89.
VASHISHTA, P., KALIA, R. K., AMTONIA, G. A., and EBBSJÖ, I., 1989a, *Phys. Rev. Lett.*, **62**, 1651.
VASHISHTA, P., KALIA, R. K., EBBSJÖ, I., 1989b, *Phys. Rev.*, B, **39**, 6034.
WAGNER, T., KASAP, S. O., and MAEDA, K., 1997, *J. Mat. Res.* **12**, 1892.
WUNDERLICH, B., JIN, Y., and BOLLER, A., 1994, *Thermochim. Acta*, **238**, 227.
ZHANG, M., and BOOLCHAND, P., 1994, *Science*, **266**, 1355.